Solvent Exchange of Buried Water and Hydrogen Exchange of Peptide NH Groups Hydrogen Bonded to Buried Waters in Bovine Pancreatic Trypsin Inhibitor†

Erik Tüchsen,‡ J. M. Hayes,§ S. Ramaprasad,‖ Valerie Copie,⊥ and Clare Woodward*

Department of Biochemistry, University of Minnesota, St. Paul, Minnesota 55108

Received October 7, 1986; Revised Manuscript Received March 19, 1987

ABSTRACT: Solvent exchange of ^{18}O-labeled buried water in bovine pancreatic trypsin inhibitor (BPTI), trypsin, and trypsin–BPTI complex is measured by high-precision isotope ratio mass spectrometry. Buried water is labeled by equilibration of the protein in ^{18}O-enriched water. Protein samples are then rapidly dialyzed against water of normal isotope composition by gel filtration and stored. The exchangeable ^{18}O label eluting with the protein in 10–300 s is determined by an H_2O–CO_2 equilibration technique. Exchange of buried waters with solvent water is complete before 10–15 s in BPTI, trypsin, and BPTI–trypsin, as well as in lysozyme and carboxypeptidase measured as controls. When in-exchange dialysis and storage are carried out at pH ≥2.5, trypsin–BPTI and trypsin, but not free BPTI, have the equivalent of one ^{18}O atom that exchanges slowly (after 300 s and before several days). This oxygen is probably covalently bound to a specific site in trypsin. When in-exchange dialysis and storage are carried out at pH 1.1, the equivalent of three to seven ^{18}O atoms per molecule is associated with the trypsin–BPTI complex, apparently due to nonspecific covalent ^{18}O labeling of carboxyl groups at low pH. In addition to ^{18}O exchange of buried waters, the hydrogen isotope exchange of buried NH groups H bonded to buried waters was also measured. Their base-catalyzed exchange rate constants are on the order of NH groups that in the crystal are exposed to solvent (static accessibility > 0) and hydrogen-bonded main chain O, and their pH_{min} is similar to that for model compounds. The pH dependence of their exchange rate constants suggests that direct exchange with water may significantly contribute to their observed exchange rate.

The presence of interior water is a common, though not universal, feature of the crystal structures of globular proteins (Finney, 1979; Finney et al., 1982; Edsall & McKenzie, 1983; Baker & Hubbard, 1984). Buried water may appear as individual molecules or as hydrogen-bonded networks. Each internal water molecule makes three to four hydrogen bonds to polar groups, usually peptide O atoms and NH groups or, less often, side chain groups. These line the interior surface of the water-containing cavities at locations too distant to permit direct intramolecular H bonding. The water molecules mediate H bonds between them, even when there is not an even number of protein donors and acceptors. The buried waters thus reduce the destabilizing effects that would arise from otherwise unbonded donors and acceptors in the protein interior or at the intermolecular interface of associating proteins (Finney, 1979; Edsall & McKenzie, 1983). In the case of proteins whose structures have been determined from different crystal forms, internal waters appear at the same sites (Wlodawer et al., 1984; Deisenhofer & Steigemann, 1975; Bode & Schwager, 1975; Chambers & Stroud, 1979).

These observations strongly suggest that buried waters are essential for the stability of folded proteins, and occluded water molecules observed in protein crystals are regarded as an integral part of the protein's tertiary structure in solution as well as in the crystal. However, it is clear from neutron diffraction experiments that buried water molecules do exchange with solvent water molecules (Kossiakoff, 1982; Wlodawer et al., 1984). There are limited data on the time scale for exchange of buried waters. Neutron diffraction studies show that buried waters in protein crystals exchange with solvent on the 6–12-month time scale, even when not all of the peptide NH's have exchanged (Kossiakoff, 1982; Wlodawer et al., 1984). Other than that, one study of [^{18}O]-water exchange in chymotrypsin solutions shows that exchange of buried water is complete by about 20 min (Weber et al., 1974).

The exchange of buried water in proteins is of interest to the question of the mechanism of hydrogen isotope exchange of buried peptide hydrogen atoms with solvent hydrogen atoms (Woodward et al., 1982). As with exchange of peptide hydrogen atoms, exchange of buried water molecules implies that folded proteins undergo internal motions to provide access of buried regions to solvent. While, on the average, an interior water site in the crystal structure is occupied by a water molecule, some conformational mechanism exists for its exposure to solvent water.

We have investigated the solvent-exchange time of buried [^{18}O]water in BPTI,[1] trypsin, and trypsin–BPTI and the ^1H–^2H exchange rate constants of peptide NH's that are buried and H bonded to internal waters in the BPTI crystal structure.

† This work is supported by grants from NIH (GM26242), the University of Minnesota Graduate School, and NASA (NGR 15-003-118).

‡ Present address: Roskilde University Center, DK 4000, Roskilde, Denmark.

§ Biogeochemical Laboratories, Departments of Chemistry and of Geology, Indiana University, Bloomington, IN 47405.

‖ Present address: NMR Facility, College of Basic Sciences, Louisiana State University, Baton Rouge, LA 70803.

⊥ Present address: Department of Chemistry, Massachusetts Institute of Technology, Cambridge, MA 02139.

[1] Abbreviations: BPTI, bovine pancreatic trypsin inhibitor; SA, relative static accessibility; NMR, nuclear magnetic resonance; COSY, two-dimensional *J*-correlated spectroscopy; NOE, nuclear Overhauser effect; BAPNA, N^{α}-benzoyl-DL-arginine-*p*-nitroanilide.

0006-2960/87/0426-5163$01.50/0 © 1987 American Chemical Society

Exchange of buried water from BPTI is completed by 15 s. Similarly, buried water exchanges from the trypsin–BPTI complex before 10 s except for oxygen equivalent to one atom and associated with trypsin. Although buried waters mix rapidly with solvent waters, the hydrogen-exchange properties of cavity surface NH groups that are H bonded to buried water and of external surface NH groups that are H bonded to solvent water indicates some differences in protein–water interactions at the two surfaces.

Materials and Methods

Water containing 95% ^{18}O was purchased from Monsanto Research Corp. and BPTI from Novo Industries, Denmark. Porcine trypsin (1–5% calcium acetate by weight), lysozyme, and carboxypeptidase (crystal suspension in water) were purchased from Sigma.

Water-exchange experiments were carried out on free BPTI, free trypsin, the BPTI–trypsin complex, and as a control, lysozyme and carboxypeptidase. The protein samples were first equilibrated with [^{18}O]water and then transferred to solvent of natural isotope composition by rapid gel filtration. The time required for the filtration step was regulated to give times of 9–300 s for the period between the application of the sample to the gel and the elution of the protein fraction from the gel. The variation of this exchange time gives a rough measurement of the kinetics of ^{18}O exchange from the equilibrated protein.

Equilibration of porcine trypsin (9 mM) was carried out in [^{18}O]water buffered with 0.1 M sodium phosphate. The pH of the solution was adjusted to 2.5, and the solution was incubated for 18 h at 5 °C. Prior to the exchange experiments, pH was readjusted to 7.0 by addition of concentrated ammonia in natural water. Isotope dilution was <3%. For the equilibration of BPTI, the protein was dissolved in [^{18}O]water (0.1 M phosphate) at pH 5.5 and heated for 5 min to 90 °C in a sealed 5 × 50 mm vial. Prior to the exchange experiments, the pH was adjusted to 7.0 or 1.0 by addition of concentrated ammonia or HCl. The dilution of the isotope by introduction of natural water was <2%. Equilibration of lysozyme (10 mM) was carried out in [^{18}O]water buffered with 0.1 M sodium phosphate. The solution was equilibrated for 18 h at 25 °C, pH 7.0, in a sealed vial. For equilibration of carboxypeptidase the crystal suspension was centrifuged, and the crystals were rinsed twice with [^{18}O]water. The protein crystals were suspended in [^{18}O]water containing 0.1 M sodium phosphate, pH 7.0, and dissolved by adding solid KCl to a final concentration of 1 M. This solution was incubated for 1 h at room temperature before the filtration step.

Trypsin–BPTI complex was equilibrated as follows. Solutions of trypsin and BPTI, each approximately 10 mM, were made up separately in [^{18}O]water and adjusted to pH 1.5 or 2.5. Equimolar volumes of the two solutions were determined by mixing varying volumes of the two solutions and assaying for residual enzyme activity of trypsin against BAPNA at pH 8, as described by Simon et al. (1984). The volumes determined by extrapolating to zero residual activity were mixed, and a 2-fold molar excess of $CaCl_2$ was added. For solutions that had previously been adjusted to pH 1.5, the addition of $CaCl_2$ lowers the pH to 1.1. For solutions that had previously been adjusted to pH 2.5, a constant pH was maintained during addition of $CaCl_2$. After the addition of $CaCl_2$, the solutions were stored at 4 °C for 1 or 4 days until the filtration. Just before filtration, the pH of the solution was adjusted to the experimental pH by the addition of concentrated ammonia. A moderate amount of protein precipitate which formed when the pH was raised was removed by centrifugation. The total

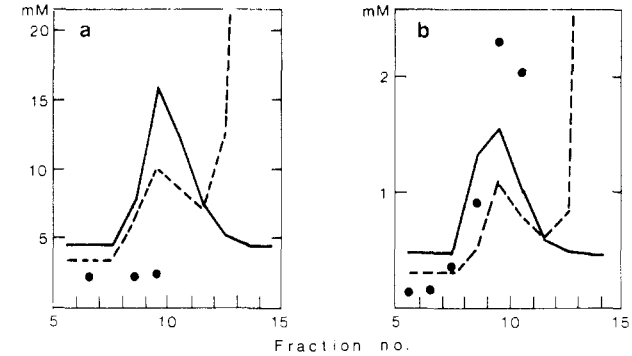

FIGURE 1: Elution profile for rapid filtration on Sephadex G25 of (a) BPTI and (b) trypsin–BPTI complex. One-drop fractions were monitored for protein concentration (—), ^{18}O enrichment of water (●), and tritium tracer (---). Tritium and ^{18}O have arbitrary scaling on the *Y* axis.

dilution of the isotope during these manipulations was 7%.

Exchange of [^{18}O]water for natural isotope abundance water was carried out by rapid filtration on Sephadex G25 (fine). Complete replacement of the water phase could be obtained in <10 s with a 4.6 × 30 mm column (0.5-mL bed volume). A 25-μL aliquot of the protein solution in [^{18}O]water was layered on top of the gel and under a 0.3 mL column of natural water buffer, while the outlet portal was closed. Within 10 s after the protein solution was layered, and by means of a quick-lock plug carrying the reservoir tubing, the cylinder was connected to an overhead buffer reservoir providing hydrostatic pressure. The quick-lock plug, designed for these experiments, is made from nylon and has a silicone-lined entry gasket for easy adjustment of the length of the reservoir tubing. The gel filtration was begun by removing the clamp at the outlet of the column, and the effluent was collected as single drop fractions, approximately 50 μL each, in small vials. The protein concentration of each fraction was determined from the absorbance at 280 nm of dilutions of 5-μL aliquots of each fraction in 300 μL of water and with the molar extinction coefficients 40 000, 5140, 44 300, 37 700 and 67 000 for trypsin, BPTI, trypsin–BPTI complex, lysozyme, and carboxypeptidase, respectively. The remainder of each drop was stored in the sealed vial until analysis of the oxygen isotope composition could be made.

The time interval between the application of the sample and the elution of the protein peak was determined in separate experiments in which the protein was replaced by Blue Dextran. The reported exchange time was taken as the time it took for the colored solution to migrate from the top to the bottom of the gel column. This time was varied between 9 and 50 s by varying the overhead hydrostatic pressure between 10 and 100 cm of water.

The capability of the column to transfer the protein between solvents of differing isotopic compositions was routinely checked by tritium tracer analysis. A relatively dilute protein solution with ~10 μCi of tritiated water was run through the column, and the fractions were analyzed by scintillation counting. Only columns capable of separating protein counts from solvent counts over a difference in count rates of 5 orders of magnitude were used. This dynamic range is similar to that required in the exchange experiment for detection of one [^{18}O]water per molecule protein in a 5 mM protein solution. The chromatographic performance of the column is shown in Figure 1.

The oxygen isotopic compositions of individual drops of water were determined by a microscale adaptation of the classical H_2O–CO_2 equilibration technique (Epstein &

Mayeda, 1953). In this procedure, oxygen atoms are allowed to exchange between CO_2 and H_2O and the oxygen isotopic composition of the water sample is determined indirectly by observation of the mass spectrum of CO_2. The ratio (O in CO_2)/(O in H_2O) is usually so small that dilution of the water oxygen by oxygen from the CO_2 can be neglected and calculations simplified. In this work, however, water samples as small as 900 μmol were equilibrated (for 48 h at 20 °C) with 20-μmol quantities of CO_2 (40 μmol of O). The accurate initial isotopic composition of the water was determined by solution of

$$F_w = [n_w F_f + 2n_e(F_e - F_i)]/n_w$$

where F terms represent fractional abundances of ^{18}O [$^{18}O/(^{16}O + ^{17}O + ^{18}O)$] and n terms represent molar quantities of water (n_w) and carbon dioxide (n_e). The subscript w refers to the initial water samples, i to initial isotopic composition of CO_2, f to final isotopic composition of the water, and e to isotopic composition of CO_2 after equilibration. Amounts of water were determined gravimetrically (±10 μg); amounts of CO_2 were determined (±1%) by PV measurement. Values of F_e and F_i were determined mass spectrometrically by using a Finnigan MAT Delta E mass spectrometer located in the Biogeochemical Laboratories at Indiana University. Calculations were carried out according to the method of Santrock et al. (1985), and the value of F_f was computed by using F_e and the known (Dugan et al., 1985) temperature-corrected (Friedman & O'Neil, 1977) isotopic fractionation factor for the CO_2–H_2O equilibrium.

The number of atoms of ^{18}O per molecule of protein, N, is given by

$$N = 55(F_x - F_0)/C$$

where the subscript x refers to water from a protein-containing fraction from the filtration column, C is the concentration (millimolar) of protein in that fraction, and the subscript 0 refers to a blank (protein-free fraction) from the same experiment. Because the F terms have dimensions equivalent to (moles of ^{18}O)/(mole of H_2O), the factor 55 (moles of H_2O/liter of H_2O) is required in the numerator.

The ^1H NMR resonances of Tyr-10, Cys-14 and Lys-41 NH's in BPTI are studied in spectra of selectively ^1H-labeled samples prepared by procedures similar to those reported for BPTI surface protons (Tüchsen & Woodward, 1985a, 1987a,b). The partial labeling procedure and assignment of Lys-41 NH is described by Tüchsen and Woodward (1987b). Due to overlap with Arg-53 NH resonances at pH 2.5–4.5, Lys-41 NH exchange rates cannot be determined from one-dimensional spectra inside this pH interval. The resonances for Tyr-10 and Cys-14 NH were both known to be overlapped by faster and slower exchanging resonances (Tüchsen & Woodward, 1985a; 1987b; Wagner & Wüthrich, 1982). Tyr-10 NH resonance at 7.78 ppm (pH 2.3) coincides with the much slower exchanging Asn-24 NH and the faster exchanging Cys-38 NH and Asn-44 $N^{\delta}H_E$. Cys-14 NH resonance at 8.9 ppm overlaps with the much slower exchanging Gln-31 NH and the faster exchanging Ile-19 NH. To label Tyr-10 and Cys-14 NH, the protein was first deuteriated at all exchangeable sites by heating to 90 °C for 5 min in ^2H_2O at pH 4.5 and then lypohilized. For ^1H back-labeling, the deuteriated protein was dissolved in ^1H_2O and 0.3 M KCl and adjusted to pH 7.2 with KOH. After 30 min at 22 °C, back-exchange was stopped by readjusting pH to 3.0, followed by lyophilization. At this point, Gln-31 and Asn-24 NH's are not back-labeled; they retain ^2H label and therefore are not observed in the ^1H NMR spectrum. The partially labeled lyophilized sample is dissolved in ^2H_2O, adjusted to pH 1.3 with ^2HCl, and incubated for 3.5 h at 25 °C. This step labels a number of faster exchanging NH's with ^2H, including Cys-38 and Asn-44 $N^{\delta}H_E$. This step also reduces the intensity of Ile-19 NH resonance that overlaps the Cys-14 NH peak at 8.9 ppm to <3% of its original intensity. The sample is then adjusted to the experimental pH, and the exchange measurements are taken. A representative spectrum is given in Figure 2.

The assignment of Cys-14 at 8.9 ppm was made from the $C^{\alpha}H$–NH cross-peak in COSY spectra (data not shown). Tyr-10 cannot be differentiated from Cys-38 NH in COSY spectra because both have the same chemical shift for $C^{\alpha}H$. The assignment of Tyr-10 is based on its NH chemical shift and its relative exchange rate, which constitutes the basis for its selective ^1H labeling. The assignment of Tyr-10 NH is corroborated by the titration of the chemical shift, which changes from 7.85 to 7.78 ppm with decreasing pH (apparent pK ~4). No titration effect is expected for the Cys-38 NH chemical shift (Tüchsen & Woodward, 1987b).

The hydrogen-exchange rate constants were determined from the rate of loss of ^1H intensity of assigned peaks in the NMR spectrum of BPTI as described by Tüchsen and Woodward (1985a) using a 300-MHz Nicolet spectrometer and a 500-MHz Bruker spectrometer. Static accessibilities (SA) are relative accessibilities as defined by Lee and Richards (1971) for the N atoms of form II BPTI structure with H atoms removed. SA calculations of the N and H atoms of peptide NH groups have also been carried out. For the residues considered here, there is no difference between these cases; all are buried except Ala-25 NH, which is partially exposed at the protein surface.

The hydrogen-exchange data are analyzed by a two-process model (Woodward & Hilton, 1980; Woodward et al., 1982; Tüchsen & Woodward, 1987b), where the observed exchange rate constant for exchange of *each* NH from a native protein is the sum of the rate constants of two processes

$$k_{obsd} = k_F + k_U \quad (1)$$

k_F is the rate constant for exchange from the folded state (low activation energy process), and k_U is the rate constant for exchange of the *same* proton via global unfolding (high activation energy process). Since under some conditions $k_F \gg k_U$, while under other conditions $k_F \ll k_U$, the conformational mechanism for exchange of a given NH may switch as the pH and/or temperature are (is) changed.

The observed rate constant for exchange involving global unfolding is

$$k_{obsd} = k_U = (k_1/k_2)k_{cx} \quad (2)$$

where k_1 and k_2 are the rate constants for unfolding and refolding in the cooperative, major unfolding transition, respectively, and k_{cx} is the rate constant for the chemical-exchange step.

The observed rate constant for low activation energy exchange may be written

$$k_{obsd} = k_F = \beta k_{cx} \quad (3)$$

where β is a parameter that expresses the contribution to the observed exchange rate from dynamic conformational processes of the folded protein. The evaluation of β is different for the two models (penetration model vs. local unfolding model) that have been proposed for the dynamic conformational processes that expose protons to solvent for exchange (Tüchsen & Woodward, 1987b).

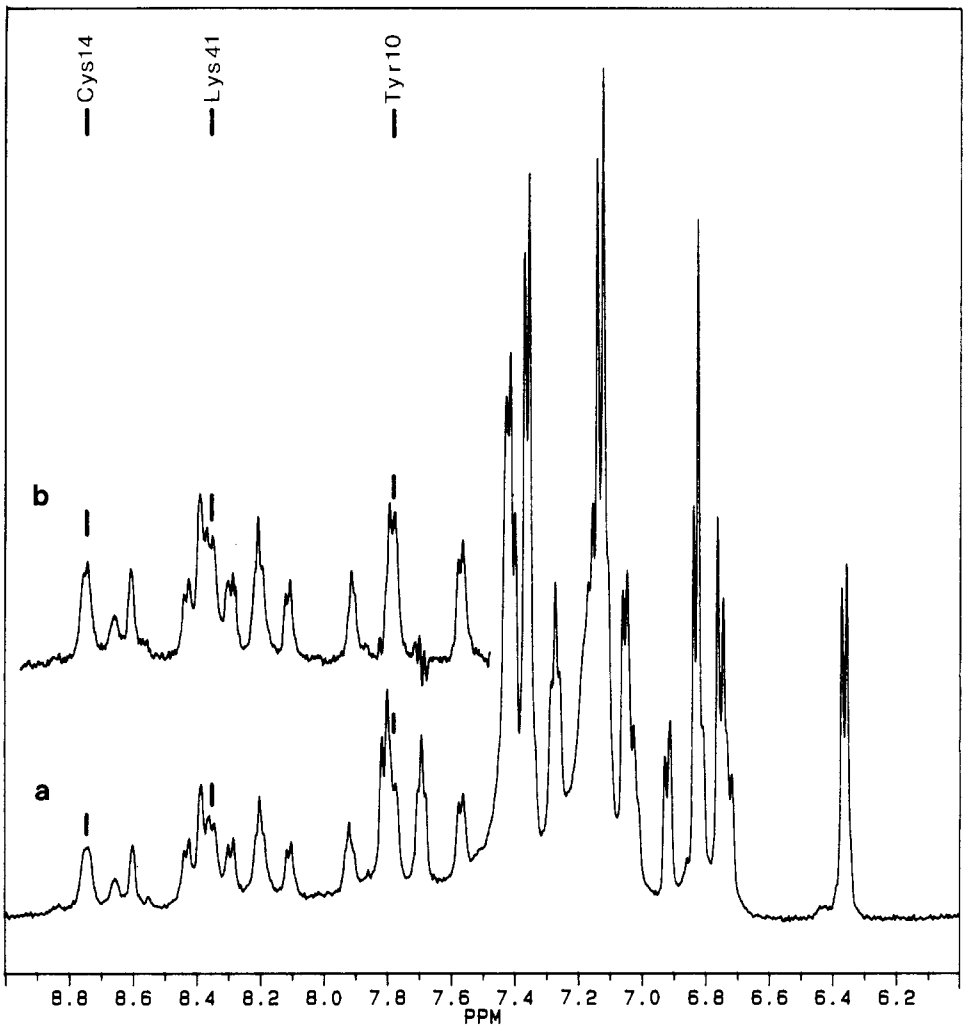

FIGURE 2: 500-MHz ^{1}H NMR spectrum of selectively ^{1}H-labeled BPTI. The protein sample was prepared as described under Materials and Methods. Spectrum a was recorded at pH 2.3. Exchange difference spectrum b was obtained by subtraction of a spectrum of fully deuteriated BPTI from a spectrum taken at pH 1.

The value of the chemical-exchange rate constant, k_{cx}, is obtained from model compounds, often poly(DL-alanine):

$$k_{cx} = k_H[H^+] + k_{OH}[OH^-] + k_0 \quad (4)$$

where k_H and k_{OH} are rate constants for acid- and base-catalyzed exchange and k_0 is for direct exchange with water. When the first two terms on the right are equal, k_{cx} goes through a minimum with pH. The pH at the minimum, pH_{min}, is a function of the relative values of k_H and k_{OH} (Tüchsen & Woodward, 1987b). The rate constant at pH_{min} is called k_{min}. For poly(DL-alanine), $k_{min} \approx 0.1$ min^{-1} and $pH_{min} \approx 3$.

Our hydrogen-exchange data are expressed as the observed rate constant at specified pH and temperature, k_{obsd}, and the values of $k_{H,obsd}$, $k_{OH,obsd}$, and $k_{0,obsd}$ derived from

$$k_{obsd} = k_F = k_{H,obsd}[H^+] + k_{OH,obsd}[OH^-] + k_{0,obsd} \quad (5)$$

where $k_{H,obsd} = \beta_H k_H$, $k_{OH,obsd} = \beta_{OH} k_{OH}$, $k_{0,obsd} = \beta_0 k_0$, and the β terms represent the effects of protein conformation on the exchange rate constant (Tüchsen & Woodward, 1987b).

RESULTS

[^{18}O]Water Exchange. BPTI contains four buried water molecules. We have examined the exchange of these with solvent water and the isotope exchange of the peptide amide protons H bonded to these waters. For the water-exchange experiments, rather than studying only free BPTI, we carried out more extensive measurements on the porcine trypsin–BPTI complex as well. The rationale for this is 3-fold. First, the complex contains the largest number of buried waters known for a single protein species, about 35 molecules. Second, the extraordinarily stable complex could be expected to stabilize the constituent proteins and perhaps slow the exchange of buried water. Third, porcine trypsin is more soluble than the bovine enzyme, allowing us to make the water-exchange measurement with higher concentrations of complex than are possible with bovine trypsin. The bovine trypsin–BPTI complex has >35 buried water molecules, 4 in BPTI, about 25 in trypsin, and 6–8 that mediate H bonds between enzyme and inhibitor atoms at the enzyme–inhibitor interface (Bode et al., 1976; Finney, 1979; Edsall & McKenzie, 1983). Since serine proteases in general have buried water networks similar to those in bovine trypsin (Edsall & McKenzie, 1983), we expect that, like bovine trypsin complex, the porcine trypsin–BPTI complex has about 35 buried water molecules.

For the water-exchange experiments, the protein is equilibrated in [^{18}O]water and transferred to natural isotope abundance water by rapid filtration on Sephadex. The Sephadex fractions are analyzed for ^{18}O eluting with the protein. For this procedure to be reliable, the protein peak must be resolved from the trailing ^{18}O solvent and the concentration of protein in the peak fraction(s) must be high enough to allow detection of one molecule of water per molecule of protein. To demonstrate the performance of the column, tritiated water, as well as [^{18}O]water is used, as shown

Table I: ^{18}O Atom Content and Protein Fractions from a 15-s Gel Filtration

protein	equilibration conditions	filtration pH	protein concn[a] (mM)	F_0[b] ($\times 10^{-3}$)	F_x[c] ($\times 10^{-3}$)	N[d]
BPTI	pH 5.5, 90 °C, 5 min	7.0	3.38	1.9866	1.9865	0.0
			9.73		1.9875	0.0
BPTI	pH 5.5, 90 °C, 5 min	1.0	2.50	1.9859	1.9862	0.0
			7.56		1.9909	0.0
trypsin	pH 2.5, 5 °C, 18 h	7.0	0.95	1.9858	2.0110	1.5
			2.07		2.0489	1.7
trypsin	pH 2.5, 5 °C, 18 h	1.0	0.72	1.9929	2.0060	1.5
			2.50		2.0719	1.9
			1.84		2.0858	3.0
lysozyme	pH 7, 25 °C, 18 h	7.0	0.64	1.9866	1.9866	0.0
			2.81		1.9866	0.0
			1.96		1.9866	0.0
carboxypeptidase	pH 7, 25 °C, 1 h	7.0	0.90	1.9856	1.9874	0.1
			0.77		1.9956	0.7

[a] The protein concentration of protein-containing fractions from gel filtration, with a standard error of ±0.05, ±0.01, ±0.01, and ±0.005 mM for BPTI, trypsin, lysozyme, and carboxypeptidase, respectively. [b] F_0 is the fractional abundance of ^{18}O [$^{18}O/(^{16}O + ^{17}O + ^{18}O)$] in a non-protein-containing blank from the same filtration. [c] F_x is the fractional abundance of ^{18}O in each protein-containing fraction. [d] N is the number of atoms of ^{18}O per molecule of protein in each protein-containing fraction.

Table II: ^{18}O Atom Content of Trypsin–BPTI Fractions from Rapid Gel Filtration[a]

equilibration conditions		filtration conditions					
pH	time (days)	pH	time (s)	protein concn (mM)	F_0 ($\times 10^{-3}$)	F_x ($\times 10^{-3}$)	N
1.1	1	7.0	9	0.05	1.9844	1.9863	2.0
				1.27		2.0150	1.3
				0.83		2.0207	2.4
1.1	1	7.0	15	0.85	1.9866	1.9967	0.8
				1.07		2.0200	1.8
				0.51		2.0149	3.3
1.1	1	7.0	26	0.79	1.9855	2.0029	1.2
				1.20		2.0148	1.3
				0.47		2.0027	2.0
1.1	1	7.0	30	0.03	1.9840	1.9852	1.3
				0.84		2.0002	1.0
				0.99		2.0116	1.5
				0.61		2.0034	1.7
1.1	1	7.0	45	0.07	1.9872	1.9883	0.9
				1.13		2.0056	0.9
				0.62		2.0068	1.7
1.1	1	7.0	90	0.10	1.9865	1.9875	0.6
				1.16		2.0102	1.1
				0.87		2.0104	1.5
1.1	4	1.1	10	0.58	1.9853	2.0216	3.4
				1.53		2.0762	3.3
1.1	4	1.1	15	0.82	1.9849	2.0889	7.0
				1.40		2.1012	4.6
1.1	4	2.5	15	0.32	1.9849	1.9928	1.4
				0.97		2.0170	1.8
				1.28		2.0281	1.9
1.1	4	4.0	15	0.25	1.9862	1.9906	1.3
				1.53		2.0237	1.4
1.1	4	7.0	15	0.16	1.9852	1.9854	0.1
				1.35		2.0074	0.9
2.5	1	7.0	20	1.08	1.9849	2.0019	0.9
				1.18		2.0117	1.3
				0.38		1.9977	1.8
2.5	1	7.0	30	0.63	1.9844	1.9929	0.8
				0.77		2.0070	1.6
				0.99		2.0059	1.2
				0.31		1.9999	2.7
2.5	1	7.0	300	1.10	1.9863	1.9973	0.6
				1.44		2.0106	0.9
				0.92		2.0041	1.1
1.1[b]	4	7.0	20	0.91	1.9851	1.9871	0.1
				1.14		1.9922	0.3
				0.58		1.9890	0.4

[a] Notations are defined in the legend to Table I. All equilibrations were carried out at 4 °C. The standard error in protein concentrations is ±0.01 mM. [b] In this sample, the water was removed from the protein within an hour after the filtration rather than several days after the filtration as in the other samples.

in Figure 1. In each filtration there are one to three 50-μL protein-containing fractions well separated from the trailing solvent, with protein concentration in the millimolar range. An enrichment of 1 mM ^{18}O over natural abundance is easily within the detection limits of the isotope ratio mass spectrometer used here.

The results of the [^{18}O]water-exchange experiments are shown in Tables I and II. Each entry refers to a single gel

filtration at specified conditions of equilibration and filtration. Within each entry there is a set of values for protein concentration, F_x, and N for each fraction in the protein peak for that filtration. The fractions are listed in the order that they elute from the Sephadex column. The protein-containing fractions obtained from each filtration provide multiple determinations of N, the molar ratio of ^{18}O to protein. Further, since the protein concentration of each fraction varies, the constancy of N for fractions from the same filtration serves as an internal quality indicator for each filtration. In general, N values for fractions before and at the protein peak are in good agreement and are considered most reliable. Higher N values for fractions after the protein peak are considered to be due to overlap with the trailing solvent peak and are disregarded in the discussion and interpretation (e.g., the last N values for trypsin at pH 1 in Table I and for trypsin–BPTI in the second entry of Table II).

Table I gives the results for uncomplexed BPTI and trypsin and, for comparison, lysozyme and carboxypeptidase. Lysozyme has four internal waters (Blake et al., 1983) in its crystal structure, while carboxypeptidase has 24 (Rees et al., 1983). BPTI and lysozyme have no detectable ^{18}O eluting with the protein. For trypsin, $N \sim 1.5$, and for carboxypeptidase, $N < 1$.

N values for the trypsin–BPTI complex are given in Table II. The pH was varied over the range 1–7 because at pH 7 the complex has an association constant of $>10^{13}$, while at pH <4 the complex is essentially dissociated and the solution consists of a mixture of the free proteins. If there were any slowly exchanging buried waters at the complex interface at pH 7, they would exchange rapidly in the dissociated complex at pH <4.

For the trypsin–BPTI complex, N is about 1.5 when the Sephadex filtration step is carried out at pH >2.5 (Table II). However, when filtration is carried out at pH 1.1, N is in the range 3–7. In interpreting these results, it must be borne in mind that the actual measurement of ^{18}O abundance is determined on water in the filtrate fractions containing protein, not on the protein itself. Each experiment has four steps: (1) equilibration with [^{18}O]water at the pH indicated, (2) gel filtration for rapid dialysis of the protein into natural abundance water, (3) storage of the filtrate in sealed vials at the pH of the filtration until the ^{18}O content of the solvent is measured, and (4) the ^{18}O measurement. Except for the last entry, step 3 for the experiments listed in Table II involved storage for several days before the isotope ratio measurement.

It is most likely that the large N values for the samples equilibrated and filtrated at pH 1.1 are due to exchange of oxygen in carboxyl groups. Covalent exchange of ^{18}O is expected during the equilibration at pH 1.1 (Murphy & Clay, 1979). However, this would be observed in these experiments only when filtration and, more importantly, storage are also carried out at pH 1.1. Oxygen that goes into carboxyl groups in days at pH 1.1 will back-exchange in days at pH 1.1, but not at pH ≥2.5, where covalent exchange of carboxyl oxygen is much slower. Stated another way, covalent in-exchange at multiple O sites occurs in equilibrations carried out at pH 1.1 for 1–4 days, and out-exchange of the label back into the solvent water similarly occurs in several days when the samples are stored at pH 1.1. However, when samples equilibrated at pH 1.1 are filtered and then stored at pH ≥2.5, ^{18}O in-exchanged at pH 1.1 is not released on the day time scale.

To test this interpretation, a control experiment was carried out. The complex was equilibrated at pH 1.1 for 4 days and then filtered at pH 1.1. However, step 3 was varied. The protein fractions were not stored for several days, but instead the water in each fraction was separated from the protein within an hour. This was done by trapping the water sublimed from the fractions soon after filtration. The results, the last entry in Table II, show that if the water is separated from the protein within an hour of the filtration, only about 0.3 ^{18}O atom per protein molecule is released into the water. This indicates that the large values of N observed for the complex equilibrated, filtered, and *stored* at pH 1.1 arise from slow out-exchange of ^{18}O during storage. The slowly exchanging ^{18}O most likely involves covalent labeling of carboxyl oxygens which occurs at pH 1.1 on the day time scale and at a very much slower rate at pH ≥2.5. This is supported by the observation that trypsin equilibrated at pH 2.5, but filtered and stored at pH 1.1, has an N of about 1.5; see Table I.

The last experiment in Table II gives a background reading, 0.3. Subtraction of 0.3 from the observed N values for trypsin–BPTI labeled at pH 1.1 gives the equivalent of approximately one oxygen atom per protein molecule, not associated with nonspecific carboxyl labeling and not released from the protein after 90 s. The observation that about one molecule of ^{18}O per molecule complex is labeled after equilibration at pH 2.5 and not released after 300 s (Table II) also indicates that one atom of oxygen in the complex is exchanged by a reaction different from the nonspecific carboxyl labeling at pH 1.1 discussed above. Since the N values are about 1.5 for free trypsin, but not for free BPTI (Table I), we conclude that the tightly bound oxygen atom is located on the trypsin molecule. Further, since this O atom elutes with the protein after 300 s, it is apparently far more tightly bound than buried waters. This suggests that one ^{18}O atom is covalently exchanged at a specific site in trypsin differentiated from nonspecific carboxyl sites by the pH dependence of its exchange which occurs in days at pH ≥2.5.

Peptide Amide Hydrogen Exchange. Buried NH groups H bonded to buried water-111, -112, -113, and -122 in BPTI crystals are peptide NH's of Tyr-10, Cys-14, Cys-38, and Lys-41, and Asn-44 $N^{\delta}H_E$, as given in Table III (Wlodawer et al., 1986). For all of these the relative static accessibility of the backbone NH group is 0. Ala-25 NH (SA = 0.53) is hydrogen bonded to water-143, which is only partially exposed to the surface. With W-143 in place in the crystal structure, Ala-25 NH has SA = 0, and SA for the W-143 molecule is <0.1. The observed exchange rate constants for Tyr-10, Cys-14, and Lys-41 are given in Table IV. Exchange kinetics of Ala-25 have been reported (Tüchsen & Woodward, 1985a). The Cys-38 NH resonance, which overlaps with Tyr-10 NH, has been eliminated from the spectra by the labeling procedure, and its exchange kinetics have not been obtained. The reso-

Table III: Hydrogen-Bond Donors and Acceptors of Buried Water Molecules in the BPTI Crystal Structure[a]

water molecule	H-bond acceptor	H-bond donor
W-111	Pro-8 O (2.7 Å)	W-112 (2.9 Å)
	Glu-7 $O^{\epsilon 2}$ (2.6 Å)	
W-112	Asn-43 O (2.8 Å)	W-113 (2.6 Å)
	W-111 (2.9 Å)	Tyr-10 NH (2.9 Å)
W-113	Tyr-10 O (2.9 Å)	Lys-41 NH (3.0 Å)
	W-112 (2.6 Å)	Asn-44 $N^{\delta}H_E$ (2.9 Å)
W-122	Cys-38 O (2.8 Å)	Cys-14 NH (3.1 Å)
	Thr-11 O (2.8 Å)	Cys-38 NH (3.1 Å)
W-143	Tyr-23 O (2.9 Å)	Ala-25 NH (3.3 Å)

[a] Hydrogen bonds (A. Wlodawer, personal communication) are for BPTI form II crystals (Wlodawer et al., 1984, 1987). The criteria for H bonds between donor XH and acceptor Y are an X–Y distance of ≤3.3 Å and an X–H–Y angle of ≥120°. X–Y distances are given in parentheses.

Table IV: Hydrogen-Exchange Rate Constants, k_{obsd} (in 10^{-3} min^{-1}), pH_{min}, k_{min}, and Catalytic Rate Constants $k_{H,obsd}$, $k_{OH,obsd}$, and $k_{0,obsd}$ at 25 °C

Tyr-10		Cys-14		Lys-41	
pH	k_{obsd}	pH	k_{obsd}	pH	k_{obsd}
1.0	0.19 (4%)[a]	0.9	0.54 (5%)	1.0	0.18 (7%)
1.5	0.095 (5%)	1.0	0.46 (2%)	1.3	0.051 (45%)
1.5	0.099 (10%)	1.5	0.12 (11%)	1.5	0.064 (24%)
2.3	0.07 (12%)	1.5	0.13 (6%)	2.3	0.033 (20%)
2.6	0.12 (24%)	2.3	0.034 (3%)	5.1	0.12 (23%)
3.8	0.097 (6%)	2.8	0.027 (17%)	6.0	5.0 (5%)
4.3	0.21 (20%)	3.4	0.055 (7%)	6.6	14 (9%)
5.3	1.9 (2%)	3.8	0.10 (16%)	7.0	29 (8%)
6.0	8.6 (8%)	4.3	0.17 (15%)		
		5.0	1.3 (30%)		
		5.3	3.4 (9%)		
		6.0	16 (12%)		

	Tyr-10	Cys-14	Lys-41
pH_{min}[d]	2.6	2.8	2.9
k_{min}[b,d]	5.6×10^{-5}	2.5×10^{-5}	(1.7×10^{-5})
$k_{H,obsd}$[c,d]	1.4×10^{-3} (40%)	4.4×10^{-3} (7%)	1.6×10^{-3} (40%)
$k_{OH,obsd}$[c,d]	1.5×10^{7} (13%)	2.2×10^{7} (20%)	4.6×10^{6} (20%)
$k_{0,obsd}$[b,d]	5×10^{-5} (50%)	9×10^{-6} (45%)	(1.3×10^{-5})[e]

[a] Relative standard error, estimated from least-squares fit of intensity vs. time data to a single-exponential rate equation. [b] k_{min} and $k_{0,obsd}$ are in min^{-1}. [c] $k_{H,obsd}$ and $k_{OH,obsd}$ are in M^{-1} min^{-1}. [d] Values and relative standard errors estimated from weighted least-squares fit of $k_{obsd} = k_{H,obsd}[H^+] + k_{OH,obsd}K_W/[H^+] + k_{0,obsd}$; $[H^+]_{min} = (k_{H,obsd}K_W/k_{OH,obsd})^{1/2}$; $k_{min} = k_{H,obsd}[H^+]_{min} + k_{OH,obsd}K_W/[H^+]_{min} + k_{obsd}$; $K_W = 10^{-15.2}$ M^2. [e] Standard error > 100%.

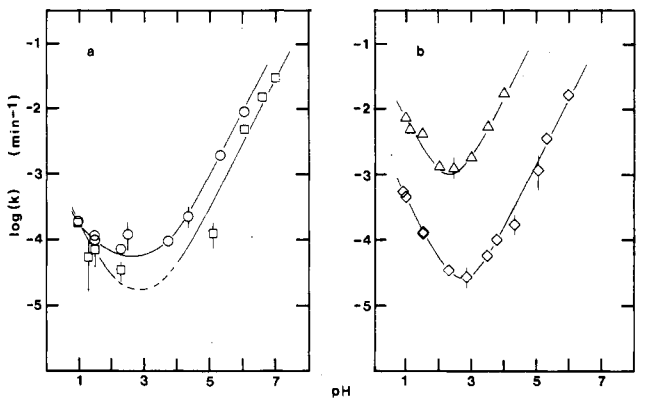

FIGURE 3: Variation of the observed exchange rate constant with pH for the NH of (a) Tyr-10 (○) and Lys-41 (□) and (b) Cys-14 (◇) and Ala-25 (△).

nance assignment of Asn-44 side chain $N^{\delta}H_E$, H bonded to buried water-113, has recently been made (Tüchsen & Woodward, 1987a), and its exchange kinetics will be reported elsewhere along with exchange data of other buried primary amide NH groups.

The pH–log rate profiles of Tyr-10, Cys-14, Ala-25, and Lys-41 are shown in Figure 3. A trend to broad and shallow shapes of the profiles in the region of pH_{min} is unlike that in similar curves for surface protons and rapidly exchanging buried protons (Tüchsen & Woodward, 1985a, 1987b). The Tyr-10 data show this feature most clearly. Also, the Lys-41 data at pH 1–3 strongly suggest a shallow pH_{min} region, but unfortunately the overlap of Lys-41 and Arg-53 NH resonances at pH 2.5–4.5 prevents unambiguous determination of the exchange rates around pH_{min}. For Ala-25, the deviation from simple acid and base catalysis is less pronounced.

Generally, when exchange data are fit to eq 5, the pH-independent term, k_0, may be neglected. A significant contribution to the observed exchange from k_0 is characterized by a broader, more shallow pH vs. log k curve in the region of pH_{min}. When the data in Figure 3 are fit to eq 5, estimates of k_0 for the peptide NH's of residues 10, 14, 25, and 41 are 5×10^{-5}, 9×10^{-6}, 4×10^{-4}, and 1.3×10^{-5} min^{-1}, respectively. The Tyr-10 NH exchange data cannot be fit to eq 5 without including a k_0 term. For Cys-14 the data are equally well fit by eq 5 with or without the k_0 term. The values of $k_{H,obsd}$, $k_{OH,obsd}$, and $k_{0,obsd}$ in Table IV are obtained with k_0 terms included in the fits. At pH_{min}, $k_{0,obsd}$ contributes 90%, 35%, 40%, and 75% to the observed rate constant, k_{min}, for Tyr-10, Cys-14, Ala-25, and Lys-41, respectively. Comparing these with model compounds, poly(DL-alanine) has $k_0 \approx 2 \times 10^{-2}$ min^{-1} (Gregory et al., 1983; Englander et al., 1979), and for *N*-methylamide, k_0 may amount to about 75% of the total exchange at pH_{min} (Hvidt et al., 1983).

Unambiguous evidence for direct exchange with water has not been reported for proteins. Broad minima for the pH vs. log rate constant of the slowest exchanging β-sheet BPTI protons at high temperature have been ascribed to uncatalyzed exchange (Gregory et al., 1983). This was based primarily on extrapolations to high temperatures of model compound data in which the activation energy for k_0 is significantly larger than that for k_H and k_{OH}, making k_0 relatively more important at high temperature. In contrast, Hvidt et al. (1983) have concluded that the relative temperature coefficients of k_0, k_H, and k_{OH} are such that the uncatalyzed exchange reaction is of increasing importance with decreasing temperature. Further, the high-temperature data for the slowest exchanging β-sheet protons of BPTI are as well explained as an effect on the high activation energy mechanism, eq 2, of a pH-induced transition between two folded forms of BPTI of differing global thermal stability (Hilton et al., 1981; Woodward et al., 1982). Exchange of the protons under consideration here is considered to involve the low activation energy mechanism, eq 3 and 5, because the apparent activation energy of Ala-25 is low (Tüchsen & Woodward, 1985a) and because the exchange rates are too fast to be associated with global unfolding rates. In addition, the pH vs. log k_{obsd} curves for the β-sheet protons deviate far more from simple acid and base catalysis than the curves in Figure 3 [cf. Figure 3 in Woodward and Hilton (1980)]. We conclude that the shallow pH minima observed here are not related to the broad minima observed for the β-sheet BPTI protons at high temperatures.

Discussion

The ^{18}O experiments, Tables I and II, indicate that buried waters in BPTI, trypsin–BPTI complex, lysozyme, and carboxypeptidase exchange before 10–15 s. This increases by about 2 orders of magnitude the slow limit for exchange rates of buried water demonstrated experimentally (Weber et al., 1974). While the buried water is a part of the protein's tertiary structure, it is clearly a dynamic component that moves in and out of the protein on a time scale of less than seconds. Rapid exchange of buried waters implies that buried protein–water hydrogen bonds are rapidly broken and reformed and that the protein internal atoms move to accommodate the exchange of buried water. It may be argued that the buried water in BPTI is not very buried and that small adjustments of side chains might account for its exchange. But this cannot be the case for the trypsin–BPTI complex, which has a number of deeply buried water molecules, including those at the protein–protein interface.

The equivalent of one oxygen atom in trypsin–BPTI is labeled by ^{18}O-labeled solvent water after 24 h at pH 1.1 and 2.5 by a reaction not involving nonspecific carboxyl oxygen exchange. The labeled oxygen is tightly bound and does not back-exchange in several minutes at pH 7, but does back-

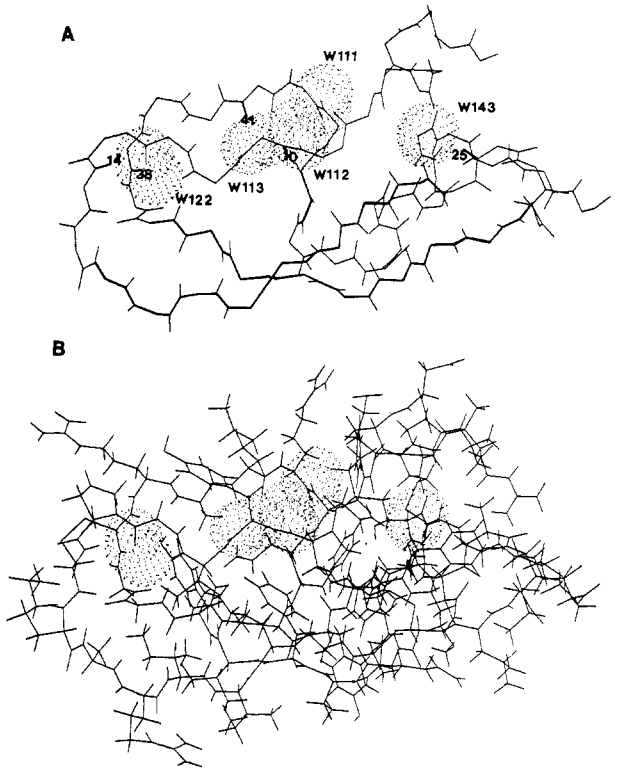

FIGURE 4: Crystal structure of BPTI and buried water molecules. (A) Backbone atoms and buried waters. Buried NH groups hydrogen bonded to buried waters are given in heavier lines and labeled at the H atoms. Backbone atoms of the β-sheet segments, located at the bottom of the molecule in this view, are also shown in heavier lines. (B) Full BPTI structure with side chains from the same view.

exchange after several days at pH 1–7. The oxygen is bound to the trypsin molecule, probably covalently, and does not represent a buried water molecule. It is likely that the labeled oxygen constitutes a single O atom at a particularly reactive site in trypsin.

Rapid exchange of buried waters implies that water-containing cavities may be considered, in essence, an extension of the exterior surface of the protein. However, differences in the dynamics of protein–solvent interactions at the internal and exterior surfaces in BPTI are indicated by differences in the hydrogen-exchange properties of cavity surface NH and external surface NH. Exchange rate constants of these two types of NH may be compared directly since mixing of buried $^2HO^1H$ with bulk water (isotope dilution after exchange) does not limit exchange of NH groups lining the water cavity. With half-times $\ll$ 10 s, the exchange rates of buried water molecules with solvent water are $\gg$2 orders of magnitude faster than hydrogen-exchange rates of NH's in model peptides at the pH_{min}.

Cavity surface NH groups are hydrogen bonded to internal waters in crystal form II BPTI, as shown in Figure 4. Water-111, -112, -113 and -122 are buried (Wlodawer et al., 1986). W-143 is nearly buried, and static accessibilities for its H_1, O and H_2 are 0, 0.06 and 0.25, respectively. Since the form II structure was solved by a joint refinement of neutron and X-ray diffraction data (Wlodawer et al., 1984) it includes hydrogen atoms. The cluster of water-111, -112, and -113 forms a H-bonded network within a deep cavity, with W-111 near the mouth of the cavity and slightly exposed to the outside (for W-111, SA is <0.02 for oxygen and 0 for the H atoms). Backbone atoms of the β-sheet sequences, residues 16–24, 27–36, and 45–46, containing the slowest exchanging protons in BPTI (Woodward & Hilton, 1980; Wüthrich et al., 1980) are indicated with heavier lines in the lower section of the molecule in Figure 4a. Buried donors and acceptors of H bonds to buried water, and the donor–acceptor interatomic distances, are given in Table III. Donor peptide NH's of residues 10, 14, 25, 38, and 41 are labeled in Figure 4a. The O atoms in the peptide groups of residues 10, 14, and 41 (oxygen of the previous residue) are exposed to the surface and H bonded to bulk waters.

Rate constants of the 54 peptide NH's in BPTI range over 8–10 orders of magnitude. In general, surface NH's are among the most rapidly exchanging. Actual exchange rate constants of external surface NH groups are distributed over several orders of magnitude, with the fast end of the distribution similar to exchange rates for small amides (Tüchsen & Woodward, 1985a,b, 1987b). Among the 21 NH groups with SA > 0, only 3 are intramolecularly H bonded to main-chain O (residues 16, 28, and 53), and these have exchange rates at the slower end of the distribution for external surface protons. For external surface peptide groups, pH_{min} values range from very low (<1.5) for some groups with exposed N and buried O, to very high (4.2) for one NH with exposed O and intramolecularly H-bonded N. The value of pH_{min} is an index of the relative magnitudes of $k_{H,obsd}$ and $k_{OH,obsd}$ (Tüchsen & Woodward, 1985b, 1987b); an increase in $k_{H,obsd}$ relative to $k_{OH,obsd}$ leads to an increase in pH_{min}. Acid-catalyzed exchange depends on the accessibility of the peptide O to H^+ catalyst and the peptide NH to water, while base-catalyzed exchange depends on the accessibility of the NH to OH^- catalyst and to water. The higher pH_{min} of intramolecularly H-bonded surface NH groups is attributed primarily to the higher SA of their peptide O as compared to their NH (Tüchsen & Woodward, 1987b).

In the comparison of exchange of external surface NH to exchange of cavity surface NH, two points can be made. First, regarding the relative exchange rates of buried NH's H bonded to buried waters, values for residues 10, 14, and 41 are similar to each other, and distinctly different from that for residue 25 (Figure 3). Ala-25 NH is H bonded to W-143, which may be thought of as a nearly buried surface water, or as a slightly exposed internal water. The faster exchange rates of Ala-25 NH, typical of surface protons not intramolecularly H bonded (Tüchsen & Woodward, 1985a), favor the former. Second, exchange rate constants for residues 10, 14, and 41, in Table IV, are clearly less than those for most surface NH's but in the range of those for the three NH groups with SA > 0 and intramolecular H bonding of the peptide NH to main-chain O. Compared to the latter, residues 10, 14, and 41 have similar k_{OH} values, somewhat smaller k_H values, and, consequently, lower pH_{min} values that are in the normal range of those for model peptides with electrostatic and inductive effects taken into account.

The observation of smaller values of $k_{H,obsd}$ and $k_{OH,obsd}$, but normal pH_{min}, leads to interesting conclusions about differences in water–protein interactions in internal cavities and water–protein interactions on the protein surface. Normal pH_{min} values for residues 10, 14, and 41 indicate that $k_{H,obsd}/k_{OH,obsd}$ is the same as that for model compounds and therefore, $\beta_H = \beta_{OH}$ (cf. eq 5). In an O-protonation mechanism, β_H expresses the effects of protein conformation on accessibility of H^+ to the peptide O and of water to NH and β_{OH} expresses effects of protein conformation on accessibility of OH^- and of water to NH (Tüchsen & Woodward, 1987b). Peptide O atoms of residues 10, 14, and 41 NH (O of residues 9, 13, and 40) are on the protein surface and H bonded to external waters in the crystal structure and presumably well exposed to solvent

H^+ in solution. Because acid-catalyzed exchange does not change *relative* to base-catalyzed exchange, the accessibility to OH^- of residue 10, 14, and 41 NH groups is the same as the accessibility of surface O to H^+. Therefore, decreased exposure to catalyst of NH groups lining the water cavity does not explain why their exchange rates are less than those for surface NH groups. Further, this is not due to slow mixing with solvent of the H-exchanged buried water molecule, as mentioned above. The slower exchange of NH groups of residues 10, 14, and 41 is most likely due to an increased stability of the H bond between buried NH and buried water and an associated increase in the residence time of individual buried water molecules at interior cavity sites as compared to surface water molecules at surface sites.

This possibility is consistent with the crystallographic temperature factors of waters in BPTI (Wlodawer et al., 1987). Buried waters, and numerous external surface waters, are observed with 100% occupancies and H bonded to protein polar atoms, including peptide NH and O. However, temperature factors for buried waters are significantly less than those for external surface waters, implying less dynamic disorder for the buried waters. Interestingly, W-143 has a temperature factor similar to that for external waters.

Greater stability of hydrogen bonds between buried NH and buried waters is also consistent with the observation that exchange data for Tyr-10, Ala-25, and Lys-41 are not well fit to simple first-order acid and base catalyses, embodied in the first two terms on the right of eq 5. The simplest explanation is that direct exchange with water is not negligible for these protons, and we take this to be the most likely.[2] A higher contribution of direct exchange with water for buried NH H bonded to buried water may be explained by a more favorable geometry of the buried water H bonds. In this regard, it may be noted that the two NH groups with the most clearly flattened minima, Tyr-10 and Lys-41, are the main-chain NH's with the shortest H-bonding distance to buried water (Table III). An additional factor contributing to a greater involvement of direct exchange with water has been suggested by Hvidt et al. (1983), namely, a change in the ionization constant of buried water as compared to solvent water. Either explanation requires that the exchanging NH interacts with water that is buried, in which case the NH, at the time of exchange, has a local conformation similar to the crystal structure and is not exposed to bulk solvent. This may be drawn in support of a penetration model for exchange from the folded state (Woodward et al., 1982; Tüchsen & Woodward, 1987b).

The dynamic aspect of buried water structure has been considered in other contexts. In molecular dynamic simulations of form I BPTI (Levitt, 1981, 1983),[3] internal waters break and re-form H bonds with various protein donors and acceptors in the vicinity, and two move about on the picosecond time scale. In penetration models of the protein dynamic structure governing hydrogen exchange, it is suggested that mobile internal waters stabilize protein structure by making transient H bonds with donors and acceptors whose H bonds are constantly breaking and re-forming as the protein fluctuates (Lumry & Rosenberg, 1975; Woodward et al., 1982; Tüchsen & Woodward, 1987b). In this regard, it is interesting to note that the buried waters in BPTI are grouped in the vicinity of the more rapidly exchanging buried NH protons and well separated from the very slowly exchanging buried NH protons in the β-sheet strands that traverse the molecule (Figure 4).

[2] Other explanations include an effect of a carboxyl titration on $k_{H,obsd}$ and/or $k_{OH,obsd}$ in the pH region of the pH_{min}.

[3] The buried waters numbered 1–4 by Levitt (1981, 1983) are numbered 112, 113, 122, and 143 in the form II structure.

ACKNOWLEDGMENTS

We thank Dr. Alexander Wlodawer for providing access to his results prior to publication and Dr. Robert Langridge for use of the molecular graphics facility at the University of California at San Francisco. We acknowledge the Danish Natural Sciences Research Council for access to the 500-MHz Bruker spectrometer, and we thank Dr. K. Bock at the Technical University, Copenhagen, for assistance.

Registry No. BPTI, 9087-70-1; H_2O, 7732-18-5; H_2, 1333-74-0; trypsin, 9002-07-7; carboxypeptidase, 9031-98-5; lysozyme, 9001-63-2.

REFERENCES

Baker, E., & Hubbard, R. (1984) *Prog. Biophys. Mol. Biol. 44*, 97.

Blake, C., Pulford, W., & Artymiuk, P. (1983) *J. Mol. Biol. 167*, 693–723.

Bode, W., & Schwager, P. (1975) *J. Mol. Biol. 98*, 693–717.

Bode, W., Schwager, P., & Huber, R. (1976) *Miami Winter Symp. 11*, 43–76.

Chambers, J., & Stroud, R. (1979) *Acta Crystallogr., Sect. B: Struct. Crystallogr. Cryst. Chem. B35*, 1861–1865.

Deisenhofer, J., & Steigemann, W. (1975) *Acta Crystallogr., Sect. B: Struct. Crystallogr. Cryst. Chem. B31*, 238–250.

Dugan, J., Borthwick, J., Harmon, R., Gagnier, M., Glahn, J., Kinsel, E., MacLeod, S., Viglino, J., & Hess, J. (1985) *Anal. Chem. 57*, 1734–1736.

Edsall, J. T., & McKenzie, H. A. (1983) *Adv. Biophys. 16*, 53–183.

Englander, J. J., Calhoun, D., & Englander, S. W. (1979) *Anal. Biochem. 92*, 517–524.

Epstein, S., & Mayeda, T. (1953) *Geochim. Cosmochim. Acta 4*, 213–224.

Finney, J. L. (1979) *Water: Compr. Treatise 6*, 47–122.

Finney, J. L., Goodfellow, J. M., & Poole, P. L. (1982) in *Structural Molecular Biology: Methods and Applications* (Davies, D. B., Ed.) pp 387–426, Plenum, New York.

Freidman, I., & O'Neil, J. (1977) *Compilation of Stable Isotope Fraction Factors of Geochemical Interest*, U.S. Geological Survey Professional Paper 440-K, U.S. Geological Survey, Alexandria, VA.

Gregory, R., Carbo, L., Percy, A., & Rosenberg, A. (1983) *Biochemistry 22*, 910–917.

Hilton, B., Trudeau, K., & Woodward, C. (1981) *Biochemistry 20*, 4697–4703.

Hvidt, A., Gesmer, H., & Led, J. (1983) *Acta Chem. Scand., Ser. B B37*, 227–234.

Kossiakoff, A. A. (1982) *Nature (London) 296*, 713–721.

Lee, B., & Richards, F. M. (1971) *J. Mol. Biol. 55*, 379–400.

Levitt, M. (1981) *Ann. N.Y. Acad. Sci. 367*, 162–181.

Levitt, M. (1983) *J. Mol. Biol. 168*, 621–657.

Lumry, R., & Rosenberg, A. (1975) *Colloq. Int. C.N.R.S. 246*, 55–63.

Murphy, R., & Clay, K. (1979) *Biomed. Mass Spectrom. 6*, 309–314.

Rees, D. C., Lewis, M., & Lipscomb, W. N. (1983) *J. Mol. Biol. 168*, 367–387.

Santrock, J., Studley, S., & Hayes, J. (1985) *Anal. Chem. 57*, 1444–1448.

Simon, I., Tüchsen, E., & Woodward, C. (1984) *Biochemistry 23*, 2064–2068.

Tüchsen, E., & Woodward, C. (1985a) *J. Mol. Biol. 185*, 405–419.
Tüchsen, E., & Woodward, C. (1985b) *J. Mol. Biol. 185*, 421–430.
Tüchsen, E., & Woodward, C. (1987a) *Biochemistry 26*, 1918–1925.
Tüchsen, E., & Woodward, C. (1987b) *J. Mol. Biol. 193*, 793–802.
Wagner, O., & Wüthrich, K. (1982) *J. Mol. Biol. 160*, 343–361.
Weber, B., Storm, M., & Boyer, P. D. (1974) *Arch. Biochem. Biophys. 163*, 1–6.
Wlodawer, A., Walter, J., Huber, R., & Sjolin, L. (1984) *J. Mol. Biol. 180*, 301–329.
Wlodawer, A., Deisenhofer, J., & Huber, R. (1987) *J. Mol. Biol. 193*, 145–156.
Woodward, C., & Hilton, B. (1979) *Annu. Rev. Biophys. Bioeng. 8*, 99–127.
Woodward, C., & Hilton, B. (1980) *Biophys. J. 32*, 561–575.
Woodward, C., Simon, I., & Tüchsen, E. (1982) *Mol. Cell. Biochem. 48*, 135–160.
Wüthrich, K., Wagner, O., Richarz R., & Braun, W. (1980) *Biophys. J. 32*, 549–560.

5′-Modified Agonist and Antagonist (2′–5′)(A)$_n$ Analogues: Synthesis and Biological Activity†

Catherine Bisbal, Michèle Silhol, Marc Lemaître, Bernard Bayard, Tamim Salehzada, and Bernard Lebleu*
Laboratoire de Biochimie des Protéines, UA CNRS 1191, Université de Montpellier II, 34060 Montpellier Cedex, France
Timothy D. Perrée and Michael G. Blackburn
Department of Chemistry, University of Sheffield, Sheffield S37H, U.K.
Received November 6, 1986; Revised Manuscript Received March 12, 1987

ABSTRACT: Two 5′-modified (2′–5′)(A)$_4$ oligomers with an increased resistance to phosphatase degradation were synthesized and evaluated for their ability to develop an antiviral response when introduced into intact cells by microinjection or by chemical conjugation to poly(L-lysine). The enzymatic synthesis of 5′-γ-phosphorothioate and β,γ-difluoromethylene (2′–5′)(A)$_4$ from adenosine 5′-*O*-(3-thiotriphosphate) and adenosine β,γ-difluoromethylenetriphosphate by (2′–5′)-oligoadenylate synthetase is described. The isolation and characterization of these (2′–5′)(A)$_4$ analogues were achieved by high-performance liquid chromatography. The structures of 5′-modified tetramers were corroborated by enzyme digestion. These two 5′-modified tetramers compete as efficiently as natural (2′–5′)(A)$_4$ for the binding of a radiolabeled (2′–5′)(A)$_4$ probe to ribonuclease (RNase) L. Nevertheless, at the opposite to 5′-γ-phosphorothioate (2′–5′)(A)$_4$, β,γ-difluoromethylene (2′–5′)(A)$_4$ failed to induce an antiviral response after microinjection in HeLa cells. In addition, it behaves as an antagonist of RNase L as demonstrated by its ability to inhibit the antiviral properties of 5′-γ-phosphorothioate (2′–5′)(A)$_4$ when both are microinjected in HeLa cells. The increased metabolic stability of 5′-γ-phosphorothioate (2′–5′)(A)$_4$ as compared to that of (2′–5′)(A)$_4$ was first demonstrated in cell-free extracts and then confirmed in intact cells after introduction in the form of a conjugate to poly(L-lysine). Indeed, 5′-γ-phosphorothioate (2′–5′)(A)$_4$–poly(L-lysine) conjugate induces protein synthesis inhibition and characteristic ribosomal RNA cleavages for longer times than unmodified (2′–5′)(A)$_4$–poly(L-lysine) in the same cell system. These observations provide evidence for an intracellular activation of RNase L by this 5′-modified (2′–5′)(A)$_4$ analogue. This stabilized (2′–5′)(A)$_n$ agonist and antagonist may be of value for further studies on the biological relevance of the (2′–5′)(A)$_n$ system. Their possible utilization in chemotherapy will be severely restricted by their narrow spectrum of antiviral activity.

The (2′–5′)(A)$_n$[1] system now appears to be a part of the antiviral response of cells to interferons (IFNs) and is thought to be involved in the control of cell growth and differentiation [see Johnston and Torrence (1984) and Silverman (1984) for recent reviews]. Agonists and antagonists of RNase L, the effector enzyme in this system, thus appear as possible tools for a better understanding of the biological relevance of the (2′–5′)(A)$_n$ system as well as for antiviral and antineoplastic chemotherapy. Use for these purposes necessitates solving certain problems such as poor penetration in intact cells and low metabolic stability of (2′–5′)(A)$_n$ oligomers. A number of methods of introduction of (2′–5′)(A)$_n$ into intact cells have

† This work has been supported by grants from the Centre National de la Recherche Scientifique (Programme Interdisciplinaire de Recherche sur les Médicaments), the Institut National de la Santé et de la Recherche Médicale, and the Association pour le Développement de la Recherche sur le Cancer. M.L. holds a long-term EMBO fellowship.
* Correspondence should be addressed to this author.

[1] Abbreviations: VSV, vesicular stomatitis virus; EMCV, encephalomyocarditis virus; m.o.i., multiplicity of infection; (2′–5′)(A)$_n$, a series of oligomers of adenylic acid with (2′–5′)-phosphate ester linkages and a triphosphate at the 5′-end, with n usually >2; "core" of (2′–5′)(A)$_n$ and its derivatives, (2′–5′)(A)$_n$ lacking the 5′-triphosphate; ATP-γ-S, adenosine 5′-*O*-(3-thiotriphosphate); ATP-β,γ-CF$_2$, adenosine β,γ-difluoromethylenetriphosphate; IFN, interferon; MEM, minimal essential medium; poly(rI)·poly(rC), poly(riboinosinic acid)·poly(ribocytidylic acid); HPLC, high-performance liquid chromatography; BAP, bacterial alkaline phosphatase; DEAE, diethylaminoethyl; RNase, ribonuclease; pfu, plaque-forming unit(s). Enzymes: bacterial alkaline phosphatase (EC 3.1.3.1); snake venom phosphodiesterase I (EC 3.1.4.1); T4 RNA ligase (EC 6.5.1.3); (2′–5′)-oligoadenylate synthetase (EC 2.7.7); (2′–5′)-(A)$_n$-dependent endoribonuclease or RNase L (EC 3.1.2.7); ribonuclease T$_2$ or T$_2$ RNase (ribonuclease 3′-oligonucleotidohydrolase from *Aspergillus oryzae*; EC 3.1.4.23).

0006-2960/87/0426-5172$01.50/0 © 1987 American Chemical Society